ACS Catalysis

Letter

pubs.acs.org/acscatalysis

Pore Structure and Bifunctional Catalyst Activity of Overlayers Applied by Atomic Layer Deposition on Copper Nanoparticles

Ana C. Alba-Rubio,[†,□] Brandon J. O'Neill,[†,□] Fengyuan Shi,[‡] Cem Akatay,[§] Christian Canlas,[⊥] Tao Li,[∥] Randall Winans,[∥] Jeffrey W. Elam,[⊥] Eric A. Stach,[¶] Paul M. Voyles,[‡] and James A. Dumesic[†,*]

[†]Department of Chemical and Biological Engineering and [‡]Materials Science Program, University of Wisconsin, Madison, Wisconsin 53706, United States

[§]School of Materials Engineering, Purdue University, West Lafayette, Indiana 47907, United States

[⊥]Energy Systems Division and [∥]X-ray Sciences Division, Argonne National Laboratory, Argonne, Illinois 60439, United States

[¶]Center for Functional Materials, Brookhaven National Laboratory, Upton, New York 11973, United States

Supporting Information

ABSTRACT: We present a model system, based on spherical nonporous supports, to facilitate the characterization of supported metal catalysts stabilized by atomic layer deposition (ALD) against sintering and leaching under liquid-phase conditions. Calcination at high temperatures (973 K) produces pores in the ALD overcoat, and we image these pores using scanning transmission electron microscopy and electron energy loss spectroscopy (STEM/EELS). We determine the size of these pores to be ~1 nm using small-angle X-ray scattering (SAXS). Finally, we demonstrate the use of ALD to synthesize novel bifunctional catalysts by the addition of an acidic oxide layer to the stabilizing overcoat.

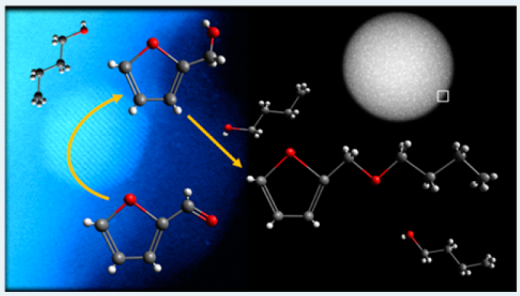

KEYWORDS: *Atomic Layer Deposition, Electron Microscopy, Catalyst Stability, Copper, Bifunctional Catalysis*

The high stability of precious-metal catalysts underlies their importance in petrochemical and biomass refining. For reasons of environmental and economic sustainability, it would be desirable to replace precious-metal catalysts (e.g., Pt) with base metals that are more earth-abundant (e.g., Cu). However, base-metal catalysts are especially susceptible to irreversible deactivation through sintering or leaching, especially under liquid-phase reaction conditions.[1−4] Accordingly, the search for base-metal catalysts that are stable under liquid-phase reaction conditions has been an important challenge in the field of heterogeneous catalysis. Recently, O'Neill et al.[5] reported that atomic layer deposition (ALD) can be employed to stabilize a base-metal catalyst for liquid-phase catalytic processing. Specifically, Cu nanoparticles were stabilized on γ-Al_2O_3 by ALD of an aluminum oxide overcoat for use in the liquid-phase hydrogenation of furfural.

Herein, we present a model system that can be used to facilitate investigation of the ALD overcoat structure that leads to catalyst stabilization and extend the functionality of the ALD overcoated catalyst architecture to include bifunctional catalyst activity. In this work, Cu nanoparticles (5 wt %) were supported on silica spheres to facilitate characterization of the materials. This spherical support has a low Brunauer−Emmett−Teller (BET) surface area (21 m^2 g^{-1}, Supporting Information (SI) Table S1) and no Barret−Joyner−Halenda (BJH) framework pore volume and can be considered a nonporous support. A graphical representation of the catalyst synthesis is shown in SI Figure S1. The catalyst was prepared by ion exchange, involving Coulombic metal−support interactions, leading to catalysts that are highly dispersed.[6] Figure 1a illustrates the high dispersion of the Cu nanoparticles after reduction ($Cu/spSiO_2$ reduced). The nanoparticles have a narrow distribution of sizes, with most of the nanoparticles being smaller than 1 nm (SI Figure S2). After reduction, the catalyst was overcoated using 30 alternating cycles of trimethylaluminum (TMA) and water, leaving the material encapsulated in an amorphous aluminum oxide overcoat ($30ALDAlO_x/Cu/spSiO_2$). Heat treatment in air at 973 K produced porosity in the overcoat, thereby providing access to the Cu particles ($30ALDAlO_x/Cu/spSiO_2$-973). After these treatments, the distribution of the particle sizes remains the same (SI Figure S2). Although aluminum oxide ALD had been used to stabilize precious metals supported on alumina,[7] base metals supported on alumina,[5] and precious metals supported on nonalumina supports,[8] to our knowledge, this is the first time that aluminum oxide ALD has been utilized for the stabilization of base-metal particles over a support that is not alumina.

Prior to ALD overcoating, the BET surface area of Cu supported on SiO_2 spheres ($Cu/spSiO_2$) was 28 m^2 g^{-1} (SI Table S1). After reduction in H_2 at 573 K, the catalyst had 34 μmol g^{-1} of surface Cu^0 sites, as titrated by N_2O flow

Received: March 13, 2014
Revised: April 9, 2014
Published: April 11, 2014

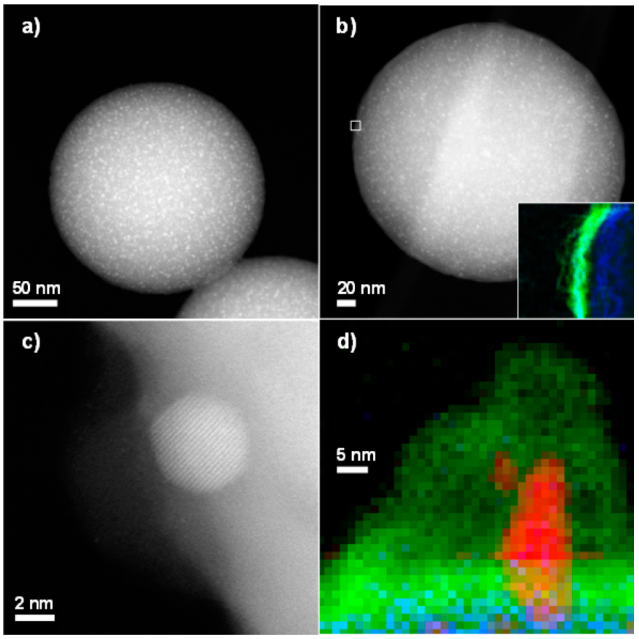

Figure 1. STEM images: (a) $Cu/spSiO_2$ reduced; (b) $30ALDAlO_x/Cu/spSiO_2$ (inset of an EDS map of the border); (c) $30ALDAlO_x/Cu/spSiO_2$, surface Cu particle overcoated by aluminum oxide; (d) EELS map of an overcoated Cu particle. Correspondence of colors and elements: green, Al; blue, Si; red, Cu.

chemisorption.[9] The surface area of the ALD overcoated sample ($30ALDAlO_x/Cu/spSiO_2$) decreased to 11 m^2 g^{-1}, indicating that the ALD process created a smooth and nonporous overcoat. Immediately after overcoating followed by reduction in H_2 at 573 K, Cu^0 sites were no longer detected by N_2O titration. Following treatment at 973 K in air ($30ALDAlO_x/Cu/spSiO_2$-973), the surface area was 12 m^2 g^{-1}, and subsequent H_2 reduction demonstrated Cu^0 surface sites (15 μmol g^{-1}) had been re-exposed. Since the overcoat layers are thin (~3.6 nm, 1.2 Å/ALD cycle), it can be inferred that the pores are not deep and are insufficient to increase the surface area;[10] however, the increase in the amount of exposed copper suggests the formation of pores. The chemisorption and surface area measurements corroborate observations of the overcoat from STEM (Figure 1b–d). Upon examination of Figure 1b, the shell of aluminum oxide surrounding the silica sphere, absent in Figure 1a, can be seen at the edges of the sphere. The composition of the overcoat was confirmed by the EDS map of the border region shown in the inset, where blue is the spherical silica support and green is the ALD aluminum oxide overcoat. Figure 1c is a high magnification image of the overcoat around a single, larger copper nanoparticle, and Figure 1d confirms by EELS that the material surrounding a different nanoparticle is the AlO_x ALD layer and not silica that had migrated during calcination.

It has been suggested that the underlying nanoparticles control the size of pores formed in the overcoat.[10] Consequently, the ~1 nm-sized copper nanoparticles in this catalyst may make the direct imaging of the porosity complicated, in contrast to the larger pores that can be seen with particles of larger size,[5] and unfortunately, direct imaging of the porosity of the ALD layer in $30ALDAlO_x/Cu/spSiO_2$-973 was not possible. We note that a rough surface was observed for $30ALDAlO_x/Cu/spSiO_2$-973, which could be an indicator of porosity. However, this roughness can also originate from damage of the sample by the electron beam, thus precluding the use of roughness as an irrefutable determinant of overcoat porosity (SI Figure S3).

To circumvent this complication, we designed a method that allows imaging of the pores by scanning transmission electron microscopy and electron energy loss spectroscopy (STEM/EELS), which is facilitated by the spherical support. The porosity of the AlO_x overcoat was probed by subsequent deposition of 20 cycles of NbO_x ALD (Figure 2). To indirectly

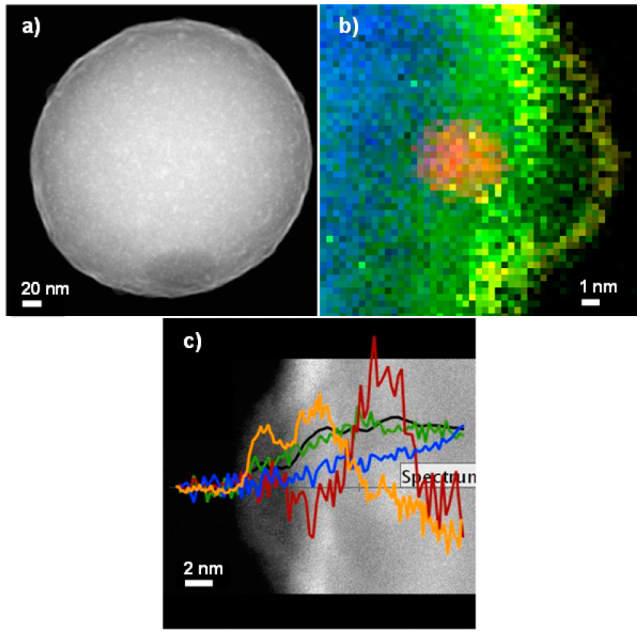

Figure 2. STEM/EELS 20 cycles of NbO_x deposited on $30ALDAlO_x/Cu/spSiO_2$: (a) STEM image, (b) EELS map at the border, (c) EELS line profile. Correspondence of colors and elements: yellow, Nb; green, Al; blue, Si; red, Cu. The black line corresponds to the high-angle annular dark field (HAADF) intensity.

image pores in the overcoat, the average penetration depth, defined as the overlap distance between the AlO_x overcoat and the center of mass of NbO_x, was calculated from EELS line scans of the catalyst (Figure 3). The value of the penetration depth should be greater than zero for all samples because the 2-D projection of STEM images makes NbO_x deposited on top of AlO_x indistinguishable from NbO_x intermixed with AlO_x. Analysis of multiple line scans revealed that the penetration depth into the AlO_x overcoat of NbO_x deposited on $30ALDAlO_x/Cu/spSiO_2$-973 (Figure 4, 2.0 ± 1.0 nm), as measured by STEM/EELS, is greater than the penetration depth of NbO_x deposited on $30ALDAlO_x/Cu/spSiO_2$ (Figure 4, 1.0 ± 0.8 nm). This result confirms the formation of porosity by calcination suggested by the N_2O chemisorption and reaction kinetics experiments (see also Figure 4 and SI Tables S1 and S2). The presence of porous features in the overcoat was also confirmed by small-angle X-ray scattering (SAXS). The changes in the high q range of 0.1–0.4 $Å^{-1}$ detected in the difference spectra for $30ALDAlO_x/Cu/spSiO_2$ and $30ALDAlO_x/Cu/spSiO_2$-973 indicate the formation of ~1 nm pores (SI Figure S4).

To ensure that our model catalyst performed comparably to our previous work, the catalyst performance was studied for the liquid-phase hydrogenation of furfural to furfuryl alcohol in 1-butanol as the solvent (403 K, 22 bar H_2). Furfural is derived

dx.doi.org/10.1021/cs500330p | ACS Catal. 2014, 4, 1554–1557

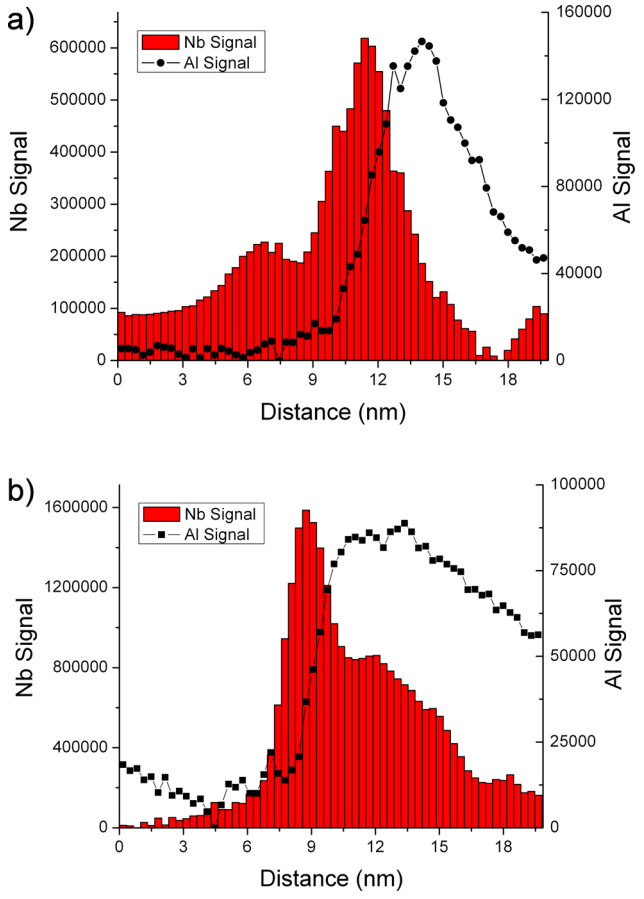

Figure 3. Example EELS line scans for NbO_x-coated (a) $30ALDAlO_x/Cu/spSiO_2$ (SI Table S2, scan 4) and (b) $30ALDAlO_x/Cu/spSiO_2$-973 (SI Table S2, scan 14).

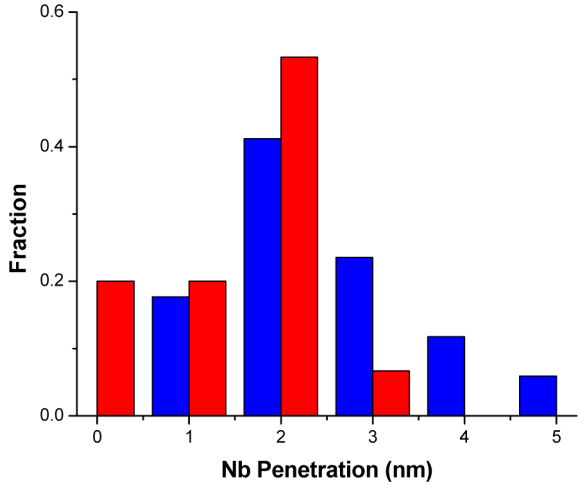

Figure 4. Penetration depth of 20 ALD cycles of NbO_x deposited in $30ALDAlO_x/Cu/spSiO_2$ (red) and $30ALDAlO_x/Cu/spSiO_2$-973 (blue) as measured by STEM/EELS. The greater penetration depth of NbO_x into the AlO_x ALD layer of $30ALDAlO_x/Cu/spSiO_2$-973 indicates the presence of pores before NbO_x deposition.

from the hemicellulose portion of biomass, and its importance is expected to increase as industries move to renewable feedstocks.[11] Furthermore, this reaction is an example of a Cu-catalyzed hydrogenation that would benefit from stabilized Cu catalysts.

Figure 5a shows that Cu/spSiO2 deactivated during time on-stream. Deactivation by the deposition of carbonaceous species on the catalyst is reversible upon regenerative calcination (673 K in air) and reduction; however, deactivation by leaching or sintering is irreversible. Figure 5a demonstrates that sintering, leaching, or both occurred because of the irreversible loss of

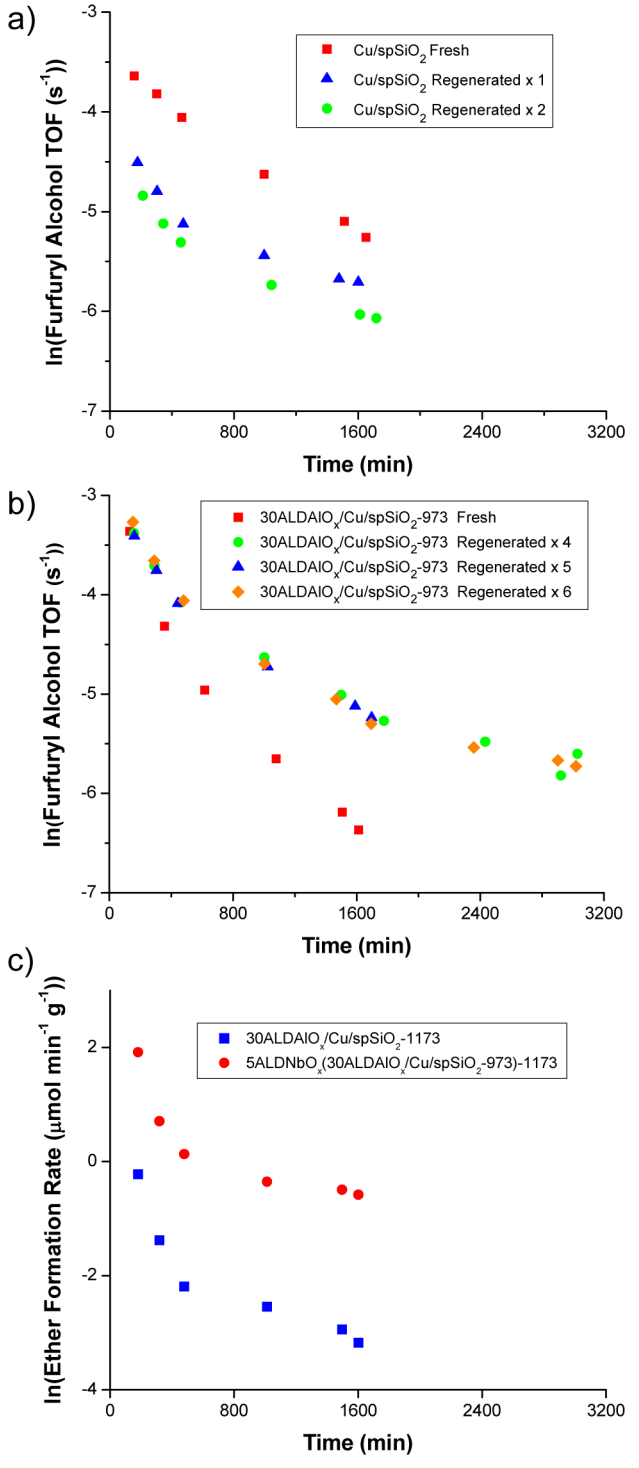

Figure 5. Furfural hydrogenation in liquid butanol at 403 K and 22 bar H_2 using (a) Cu/spSiO2 and (b) $30ALDAlO_x/Cu/spSiO_2$-973 and (c) a comparison of subsequent etherification of furfuryl alcohol with the solvent 1-butanol over $30ALDAlO_x/Cu/spSiO_2$-1173 and $5ALD-NbO_x(30ALDAlO_x/Cu/spSiO_2$-973)-1173.

dx.doi.org/10.1021/cs500330p | ACS Catal. 2014, 4, 1554−1557

activity after calcination, followed by reduction in H_2, as has been observed previously.[5]

In contrast, the overcoated catalyst (30ALDAlO$_x$/Cu/spSiO$_2$-973) demonstrated complete regeneration under the same conditions (Figure 5b). The rate per gram of this catalyst is lower than that of the catalyst previously prepared over γ-Al_2O_3,[5] but the activity per copper site is comparable (with sites counted by N_2O titration). The rate of deactivation decreased over the first few cycles, but it reaches a state that the activity and deactivation are fully regenerable. The nonporous nature of the deposited overcoat and the formation of pores upon calcination was also confirmed by the fact that there was negligible conversion on the overcoated catalyst that had not been calcined (30ALDAlO$_x$/Cu/spSiO$_2$).

In addition to nanoparticle stabilization, we note that the use of ALD overcoating allows for the synthesis of novel and finely controlled catalytic structures. The ability to add bifunctionality with atomic precision is an important and promising future area in heterogeneous catalysis, and ALD provides a potential route to achieve catalyst selectivities that rival those of biologically derived enzymatic catalysts while maintaining the robustness of inorganic heterogeneous materials. In this proof of concept example, the addition of NbO$_x$ into the pores of the 30ALDAlO$_x$/Cu/spSiO$_2$-973 followed by calcination at 1173 K (5ALDNbO$_x$(30ALDAlO$_x$/Cu/spSiO$_2$-973)-1173) leads to the formation of new acid sites capable of catalyzing the etherification of furfuryl alcohol with 1-butanol to form furfuryl butyl ether (Figure 5c) without significantly altering the amount of exposed copper (SI Table S1) or negatively affecting the activity per gram or regenerability of the furfuryl alcohol production (Figure 5S). Following the addition of 5 cycles of NbO$_x$ the rate of etherification is approximately an order of magnitude higher than that of 30ALDAlO$_x$/Cu/spSiO$_2$-1173. We also note that no furfuryl butyl ether was previously observed when the catalyst was supported on γ-Al_2O_3,[5] suggesting that the addition of AlO$_x$ via ALD to silica could also be a route to creating acidity.

We have employed a model system based on the use of nonporous supports to facilitate the detailed characterization of supported metal catalysts stabilized by ALD, and we have developed a method to indirectly image the pores in the ALD overcoat. This strategy could be useful for better imaging and understanding of other phenomena in catalysis. In addition, we have demonstrated the use of ALD to synthesize novel bifunctional catalysts.

■ ASSOCIATED CONTENT

Supporting Information

Details of synthesis, kinetic studies, and characterization. This material is available free of charge via the Internet at http://pubs.acs.org.

■ AUTHOR INFORMATION

Corresponding Author

*E-mail: dumesic@engr.wisc.edu.

Author Contributions

□A.C.A.-R. and B.J.O. contributed equally.

Notes

The authors declare no competing financial interest.

■ ACKNOWLEDGMENTS

This material is based upon work supported as part of the Institute for Atom-efficient Chemical Transformations (IACT), an Energy Frontier Research Center funded by the U.S. Department of Energy (DOE), Office of Basic Energy Sciences. C.A. acknowledges additional support from the Center for Functional Nanomaterials, Brookhaven National Laboratory, supported by the U.S. Department of Energy, Office of Basic Energy Sciences, under Contract No. DE-AC02-98CH10886. We are thankful for the use of the Advanced Photon Source, an Office of Science User Facility operated for the DOE Office of Science by Argonne National Laboratory, supported by the U.S. DOE under Contract No. DE-AC02-06CH11357. The authors acknowledge use of facilities and instrumentation supported by the University of Wisconsin Materials Research Science and Engineering Center (DMR-1121288). A.C.A.R. thanks Alex Kvit and Li He for help operating the microscope. We also thank Jean Marcel R. Gallo and Canan Sener for synthesis of the spherical silica support.

■ REFERENCES

(1) Bullock, R. M. In *Catalysis without Precious Metals*; Bullock, R. M., Ed.; Wiley-VCH Verlag GmbH & Co. KGaA: Richland, WA, 2010; pp I−XVIII.

(2) Twigg, M. V.; Spencer, M. S. *Appl. Catal., A* **2001**, *212*, 161−174.

(3) Twigg, M. V.; Spencer, M. *Top. Catal.* **2003**, *22*, 191−203.

(4) Abdulagatov, A. I.; Yan, Y.; Cooper, J. R.; Zhang, Y.; Gibbs, Z. M.; Cavanagh, A. S.; Yang, R. G.; Lee, Y. C.; George, S. M. *ACS Appl. Mater. Interfaces* **2011**, *3*, 4593−4601.

(5) O'Neill, B. J.; Jackson, D. H. K.; Crisci, A. J.; Farberow, C. A.; Shi, F.; Alba-Rubio, A. C.; Lu, J.; Dietrich, P. J.; Gu, X.; Marshall, C. L.; Stair, P. C.; Elam, J. W.; Miller, J. T.; Ribeiro, F. H.; Voyles, P. M.; Greeley, J.; Mavrikakis, M.; Scott, S. L.; Kuech, T. F.; Dumesic, J. A. *Angew. Chem., Int. Ed.* **2013**, *52*, 13808−13812.

(6) Zhou, W.; Gonzalez, R. D. *Catal. Lett.* **1992**, *12*, 73−86.

(7) Lu, J.; Fu, B.; Kung, M. C.; Xiao, G.; Elam, J. W.; Kung, H. H.; Stair, P. C. *Science* **2012**, 1205−1208.

(8) Liang, X.; Li, J.; Yu, M.; McMurray, C. N.; Falconer, J. L.; Weimer, A. W. *ACS Catal.* **2011**, *1*, 1162−1165.

(9) Chinchen, G. C.; Hay, C. M.; Vandervell, H. D.; Waugh, K. C. *J. Catal.* **1987**, *103*, 79−86.

(10) Ray, N. *Understanding pore formation in ultra-thin layers of alumina on palladium catalysts grown using atomic layer deposition*; Ph.D. Thesis, Northwestern University, 2013; p 105.

(11) Zeitsch, K. J. In *The Chemistry and Technology of Furfural and Its Many By-Products*; Elsevier: Amsterdam, The Netherlands, 2000; Vol. *13*, pp 150−155.